Molecules and Cells

EZH2-Mediated microRNA-139-5p Regulates Epithelial-Mesenchymal Transition and Lymph Node Metastasis of Pancreatic Cancer

Jin Ma[1], Jun Zhang[2], Yuan-Chi Weng[2], and Jian-Cheng Wang[2,*]

[1]Department of Gastroenterology, Luwan Branch of Ruijin Hospital Affiliated to Shanghai Jiaotong University School of Medicine, Shanghai 200020, P.R. China, [2]Department of General Surgery, Ruijin Hospital Affiliated to Shanghai Jiaotong University School of Medicine, Shanghai 200025, P.R. China
*Correspondence: jiancheng_wang@hotmail.com
http://dx.doi.org/10.14348/molcells.2018.0109
www.molcells.org

Pancreatic cancer (PC) is one of the most aggressive cancers presenting with high rates of invasion and metastasis, and unfavorable prognoses. The current study aims to investigate whether EZH2/miR-139-5p axis affects epithelial-mesenchymal transition (EMT) and lymph node metastasis (LNM) in PC, and the mechanism how EZH2 regulates miR-139-5p. Human PC and adjacent normal tissues were collected to determine expression of EZH2 and miR-139-5p, and their relationship with clinicopathological features of PC. Human PC cell line was selected, and treated with miR-139-5p mimics/inhibitors, EZH2 vector or shEZH2 in order to validate the regulation of EZH2-mediated miR-139-5p in PC cells. Dual-luciferase report gene assay and chromatin immunoprecipitation assay were employed to identify the relationship between miR-139-5p and EZH2. RT-qPCR and Western blot analysis were conducted to determine the expression of miR-139-5p, EZH2 and EMT-related markers and ZEB1/2. Tumor formation ability and *in vitro* cell activity were also analyzed. Highly-expressed EZH2 and poorly-expressed miR-139-5p were detected in PC tissues, and miR-139-5p and EZH2 expressions were associated with patients at Stage III/IV, with LNM and highly-differentiated tumors. EZH2 suppressed the expression of miR-139-5p through up-regulating Histone 3 Lysine 27 Trimethylation (H3K27me3). EMT, cell proliferation, migration and invasion were impeded, and tumor formation and LNM were reduced in PC cells transfected with miR-139-5p mimics and shEZH2. MiR-139-5p transcription is inhibited by EZH2 through up-regulating H3K27me3, thereby down-regulation of EZH2 and up-regulation of miR-139-5p impede EMT and LNM in PC. In addition, the EZH2/miR-139-5p axis presents as a promising therapeutic strategy for the treatment of PC.

Keywords: enhancer of zeste homolog 2, epithelial-mesenchymal transition, lymph node metastasis, microRNA-139-5p, pancreatic cancer, proliferation

INTRODUCTION

Pancreatic cancer (PC) is one of the leading causes of cancer-related deaths nowadays, especially in the United States, with an estimated 43,090 deaths in 2017 (Siegel et al., 2017). Invasion and migration of pancreatic cancer cells present as the two leading causes of poor prognoses in PC patients (Hartwig and Buchler, 2013; Sclafani et al., 2015). The five-year survival rate of patients with PC is only 8%, since most patients are diagnosed at advanced stages, and merely 15-20% patients are regarded eligible for surgery treatment option due to the occurrence of tumor metastases and rapid

Received 10 March, 2018; revised 11 June, 2018; accepted 13 August, 2018; published online 18 September, 2018

eISSN: 0219-1032

disease progression (Zhang et al., 2018). Therefore, there is an urgent need to explore effective biomarkers that can improve the prognostic accuracy and therapy of patients suffering from PC.

MicroRNAs (miRNAs), with their abnormal expressions in cancer cell lines, have been suggested to be closely associated with migration and invasion abilities of PC cells (Ebrahimi et al., 2016; Gayral et al., 2014). Recent evidences have demonstrated that miR-148a inhibits the migration ability of PC cells by down-regulating the expression of ErbB3 (Feng et al., 2016); miR-183 is considered as an oncogene, and a significant prognosis predictor in PC (Miao et al., 2016); moreover, miR-135b-5p is also acts as a promoter for migration, invasion and epithelial-mesenchymal transition (EMT) of PC cells (Zhang et al., 2017). Notably, miR-139-5p has been recurrently reported in cancer-related studies, and it has been documented that it serves as a potential regulatory miRNA, and is generally down-regulated in malignant neoplasms including lung cancer (Sun et al., 2015), colorectal cancer (Li et al., 2016), bladder cancer (Yonemori et al., 2016) and ovarian cancer (Wang et al., 2017); in these researches, the abnormal expression of miR-139-5p is involved in tumor progression by regulating tumor cell activities such as proliferation, apoptosis, invasion and migration. Nevertheless, the exact expression and function of miR-139-5p in PC has been yet explored.

Enhancer of zeste homolog 2 (EZH2), a histone methyltransferase, has been previously reported to interact with other PcG proteins to form a protein complex called polycomb repressive complex-2 (PRC2) (Qi et al., 2017). In various cancers, EZH2 epigenetically represses tumor suppressor gene expressions by trimethylating H3K27 and further mediates cell activities such as proliferation, apoptosis, invasion and migration (Jin et al., 2017; Siegel et al., 2017). Moreover, EZH2 is highly expressed in varying solid tumors, including PC, and its higher expression is associated with worse outcomes (Han et al., 2016; Ougolkov et al., 2008). The current study aims to identify the effect of EZH2/miR-139-5p axis on EMT and LNM of PC, and how EZH2 regulates miR-139-5p.

MATERIALS AND METHODS

Ethics statement

The current study was approved by the Ethics Committee of Ruijin Hospital Affiliated to Shanghai Jiaotong University School of Medicine. Signed informed consents were obtained from all participating patients. All animal experiments were approved by the Guide for the Care and Use of Laboratory Animal issued by National Institutes of Health, and all efforts were made to minimize the suffering of the animals included in the study.

Study subjects

A total of 105 patients diagnosed with PC by postoperative pathological examination at the Ruijin Hospital Affiliated to Shanghai Jiaotong University School of Medicine from November 2014 to September 2015 were enrolled in the current study in order to collect PC and adjacent normal tissues. A sum of 59 males and 46 females were enrolled in the study, with 58 cases of age $\geq$ 50 years old and 47 cases of age $\leq$ 50 years old; 64 cases of tumor located in the pancreatic head, and 41 located in the pancreatic tail; 26 cases of highly-differentiated PC, 43 moderately-differentiated cases and 36 lowly-differentiated cases, and 49 cases with lymph node metastasis (LNM) and 56 cases presenting without LNM. According the Union for International Cancer Control-Tumor Node Metastasis (UICC-TNM) staging system (Adsay et al., 2012), there were 34 cases at Stage II, 31 cases at Stage III and 40 cases at Stage IV. Patients who had not previously undergone drug therapy, chemoradiotherapy or immunotherapy were included in this study.

Cell culture

Various human PC cell lines, namely, SW1990, BxPC-3, PANC-1 and AsPC-1, were purchased from the Cell Bank of the Chinese Academy of Sciences (Shanghai, China). After recovery, the cells were incubated in Dulbecco's Modified Eagle Medium (DMEM) (Gibco Company, USA) containing 10% fetal bovine serum (FBS) (Gibco Company, USA) in a humidified incubator (Thermo Fisher Scientific Inc., USA) with 5% CO_2 in air at 37℃, and saturated humidity. The cells were allowed to reach 90% confluence, followed by treatment with 0.25% trypsin, and subculture at a 1 : 3 ratio. Cells presenting with the highest expression of EZH2 were selected using reverse transcription quantitative polymerase chain reaction (RT-qPCR) for further experimentation.

Immunohistochemistry

PC tissues and adjacent normal tissues were extracted from 105 included cases, and fixed with 10% formalin, dewaxed by xylene twice (10 min each time), hydrated with gradient ethanol (100%, 95%, 75% and 50%) (5 min each time), washed by distilled water for 5 min, and later rinsed with phosphate buffered solution (PBS) for 5 min. Next, the samples were supplemented with a drop of H_2O_2, followed by incubation at room temperature for 10 min and rinsing with PBS for 9 min. Then, 0.01 mol/L citrate (pH = 6.0) was added to the samples, followed by microwave retrieval for 20 min. After that, the tissues were rinsed with PBS for 9 min, added with a drop of normal goat serum and incubated at room temperature for 5 min. With the removal of serum, the sample tissues were incubated with the mouse monoclonal antibodies of EZH2 (dilution ratio of 1 : 200, ab191080, Abcam Inc., USA) at 4℃ overnight and 37℃ for 1 h. After rinsing with PBS three times (3 min each time), the samples were added with biotinylated goat anti-mouse antibodies (SPA131, Solarbio Life Sciences, China) for incubation at 37℃ for 30 min. Then, PBS rinsing was carried out three times (3 min each time) for each sample. Diaminobenzidine (DAB, Wuhan Boster Biological Technology Ltd., China) was used for color development for 1-2 min. Next, the samples were rinsed with PBS three times (2 min each time), counterstained with hematoxylin (Nanjing KeyGen Biotech Co. Ltd. China) for 1 min, dehydrated, cleared and sealed with neutral balsam. Known positive sections were used as the positive control, and PBS was regarded as the negative control in replacement of the primary antibody. The criteria for

identifying the positive expression were as follows: 5 highly magnified fields were randomly selected for counting under an optical microscope (Nikon Instech Co., Ltd, Japan), and cells presenting with brown or yellow cytoplasm were regarded as positive cells.

RT-qPCR

Total RNA content of samples was extracted using the Trizol reagent (Invitrogen Inc., USA), and then RNA integrity and purity were detected using agarose gel electrophoresis. The tested RNA fragments were regarded complete if bands 28S and 18S were bright, clear and sharp, while 28S presented with at least double the luminance of 18S. When the value of A260/A280 was between 1.8 and 2.1, the RNAs were considered as highly purified. Next, reverse transcription was carried out using a Primescript™ RT reagent Kit (RRO37A, Takara Biotechnology Ltd., China), and the steps were as follows: the RNA precipitate was firstly dissolved in 40 μl RNAase-free water, and each 200 μl pitot tube was added with 12 μl RNAase-free water, 2 μl OdT and 3 μl RNA sample for mixing. Then, the samples were heated at 70℃ for 5 min, immediately cooled in ice water for 2 min, and mixed uniformly with 1 μl deoxy-ribonucleoside triphosphate (dNTP), 1 μl guanidinium isothiocyanate, 5 μl 5 × reverse transcription buffer and 1 μl Moloney Murine Leukemia virus (MMLV) using transferpettor. Subsequently, the samples were washed in warm water at 37℃ for 90 min, heated at 70℃ for 5 min to terminate the reaction, and later placed in an ice box for preservation. Fluorescent quantitative PCR (7500, ABI Company, USA) was employed for amplification of target genes and internal reference. The PCR system included 25 μl 10 × PCR Buffer, 2.5 μl $MgCl_2$ (25 μmol/L), 1.5 μl dNTP (10 μmol/L), 0.5 μl primer (10 μmol/L), 1 μl probe (1 nmol/L), 0.25 μl Taq, 2.5 μl cDNA and 15 μl distilled H_2O. The reaction conditions were as follows: pre-denaturation at 94℃ for 5 min, 40 cycles of denaturation at 94℃ for 30 s, annealing at 58℃ for 45 s, and extension at 72℃ for 30 s, and finally extension at 72℃ for 10 min. Each reaction was repeated three times. U6 was regarded as the internal reference of miR-139-5p, and glyceraldehyde-3-phosphate dehydrogenase (GAPDH) was used as the internal reference for others. The $2^{-\Delta\Delta CT}$ method was used to calculate the relative expression levels of miR-139-5p, EZH2, N-cadherin, Vimentin and E-cadherin (Livak and Schmittgen, 2001). Ct was the number of amplification cycles when the real-time fluorescence intensity reached the set threshold. $\Delta\Delta Ct = \Delta Ct_{\text{experimental group}} - \Delta Ct_{\text{control group}}$, $\Delta Ct = Ct_{\text{target gene}} - Ct_{\text{reference gene}}$. Each experiment was repeated three times. The method was also applicable for cell experiments. PCR primers are shown in Table 1.

Dual-luciferase report gene assay

The promoter sequence and gene sequence of EZH2 along with the sequence of miR-139-5p were obtained from the National Center for Biotechnology Information (NCBI) database (http://www.ncbi.nlm.nih.gov/gene). The 3′-untranslated region (3′UTR) of EZH2 was amplified, and PCR products were cloned into pmirGLO (Promega, USA) polyclonal sites downstream of luciferase miRNA using endonuclease site Spe I and Hind III to construct pmirGLO-EZH2-wide type (Wt).

Table 1. The primer sequences of involved genes in RT-qPCR

Gene	Primer sequence
EZH2	Forward: 5′-CCCTGACCTCTGTCTTACTTGTGGA-3′
	Reverse: 5′-ACGTCAGATGGTGCCAGC AAT-3′
N-cadherin	Forward: 5′- TTTGATGGAGGTCTCCTAACACC-3′
	Reverse: 5′- ACGTTTAACACGTTGGAAATGTG-3′
Vimentin	Forward: 5′-GCACGATCCAACTCTTCCTC-3′
	Reverse: 5′-GGAGCAGAAAGCAGAACCC-3′
E-cadherin	Forward: 5′-TTCCTTCCACGAAACCAGTG-3′
	Reverse: 5′-GCCCATCTTCTTCCAGATGGTGAGC-3′
ZEB1	Forward: 5′-GATGACCTGCCAACAGACCA-3′
	Reverse: 5′-CCCCAGGATTTCTTGCCCTT-3′
ZEB2	Forward: 5′-CAAGAGGCGCAAACAAGCC-3′
	Reverse: 5′-GGTTGGCAATACCGTCATCC-3′
GAPDH	Forward: 5′-CGTCTTCACCACCATGGAGA-3′
	Reverse: 5′-CGGCCATCACGCCACAGTTT-3′
U6	Forward: 5′-TGCGGGTGCTCGCTTCGGCAGC-3′
	Reverse: 5′-CCAGTGCAGGGTCCGAGGT-3′
miR-139-5p	Forward: 5′-CCCAAAGACAAGCAGGACTC-3′
	Reverse: 5′-TGGGGTAGACTAAGGCCAGA-3′

Notes: RT-qPCR, reverse transcription quantitative polymerase chain reaction; miR-139-5p, microRNA-139-5p; EZH2, enhancer of zeste homolog 2; GAPDH, glyceraldehyde-3-phosphate dehydrogenase.

Then, the miR-139-5p binding site mutants were predicted using the target gene database, and the recombinant vector was constructed and termed the pmirGLO-EZH2-mutant type (Mut). Next, the miR-139-5p mimic or negative control (NC) was co-transfected with luciferase reporter vector into cells, with Renilla luciferase vector pRL-TK (Takara Biotechnology Ltd., China) regarded as the internal control. The relative luciferase activity was measured using a dual-luciferase Reporter Assay System (Promega Corporation, USA). Each experiment was repeated three times.

Immunofluorescence assay

Cells in the logarithmic phase of growth were selected and cultured in a 6-well plate. When cell confluence reached 60-70%, the cells were rinsed with PBS two times (3 min each time), fixed with 2.5% glutaraldehyde, and rinsed again with PBS two times (3 min each time). Then, the cells were lysed with 0.1% TritonX-100 for 5 min and rinsed by PBS two times (3 min each time). Next, the EZH2 specific antibody (ab191080, Abcam Inc., USA) was added for overnight incubation at 37℃. PBS rinsing was carried out two times (3 min each time). Then, the cells were incubated with fluorescein isothiocyanate (FITC) labeled secondary antibody for 1 h, rinsed with PBS twice (3 min each), and sealed with anti-fluorescent quenching medium. Photographs of cells were obtained using a microscope. Each experiment was repeated three times.

Chromatin immunoprecipitation (ChIP)

The EZ-Magna ChIP A kit (17-408, Millipore, Bedford, MA,

USA) was employed for ChIP assay. BxPC-3 cells (2 ml) in the logarithmic phase of growth were rinsed with precooled PBS, and ice-bathed in PBS containing Protease Inhibitor Cocktail II of equal volume for 5 min. Next, cell extracts were centrifuged at 800 g, 4℃ for 5 min to collect precipitates. Then, the cells were resuspended in 2.0 ml cell lysis buffer containing Protease Inhibitor Cocktail II and lysed on ice. Subsequently, centrifugation was carried out with 0.5 μl Protease Inhibitor Cocktail II added at 800 g, 4℃ for 5 min. The supernatant was discarded, and 2.0 ml Nuclear Lvsis Buffer was added. Later, the cells were lysed on ice, followed by supersonic decomposing to obtain fragments of 200-1000 base pairs. The groups included the positive control, NC, anti- histone 3 lysine 27 trimethylation (H3K27me3) and blank. A 50 μl DNA fragment was added with 450 μl Dilution Buffer and 2.25 μl Protease Inhibitor Cocktail II. Cells in the positive control group were supplemented with 5.0 μg of anti-Acetyl-Histone H3 antibody (ab4729, Abcam Inc., USA); those in the NC group were added with 5.0 μg of rabbit immunoglobulin G (IgG), and cells in the Anti-H3K27me3 group were added with 4.0 μg of anti-Trimethyl-Histone H3 antibody (PAB12742, Abnova, USA), and resuspended with magnetic bead-antibody complex. Then, the magnetic bead-antibody complex was washed, resuspended with 500 μl ChIP Wash Buffer before supplementation with 100 μl ChIP Elution Buffer-Protease K complex. Next, the samples were then placed on the magnetic base to collect magnetic bead-protein complex. With the removal of the supernatant, the samples were rewashed with ChIP Wash Buffer two times. DNA was extracted for further detection.

Cell grouping and transfection

Based on the design principle of shRNA, coding sequence of EZH2 was searched in the GenBank, and by adopting the online RNA interference sites given by Invitrogen, the interference sequence of shEZH2 was synthesized as (5′-CCGGCCCAACATAGATGGACCAAATCTCGAGATTTGGTCCA TCTATGTTGGGTTTTTG-3′). Next, the Blast software was applied for comparisons in the human gene group, and later identification of the only one sequence of EZH2. Endonuclease site Spe I and Hind III were cloned into p-Genesil-1 (Shanghai Beinuo Biotech Co., Ltd., China) in order to construct the p-Genesil-1-shEZH2 recombinant vector, and to verify whether the base sequence of the shRNA fragment was accurate. The PcDNA3-EZH2 vector and sequence of miR-139-3p mimic was TCTACAGTGCACGTGTCTCCAGT, and that of miR-139-3p inhibitor was ACTGGAGACACGTG CACTGTAGA, which were purchased from Shanghai GenePharma Co. Ltd., China.

BxPC-3 cells in the logarithmic phase of growth were selected. Next, the collected cell suspension was seeded in a 6-well plate (cell density of 5×10^4 cells/well), and incubated in fresh complete culture medium. Transfection was performed when cell confluence reached 50-80%, in accordance with the instructions of Lipofectamin 2000 (11668-027, Invitrogen Inc., USA). Cells were divided into the blank group, the NC group (cells transfected with irrelevant shRNA), the EZH2 vector group (cells transfected with pcDNA3-EZH2 vector with over-expressed EZH2), the shEZH2 group (cells transfected with p-Genesil-1-shEZH2 vector), the miR-139-5p mimic group (cells transfected with miR-139-5p mimic), the miR-139-5p inhibitor group (cells transfected with miR-139-5p inhibitor), and the shEZH2 + miR-139-5p inhibitor group (cells transfected with p-Genesil-1-shEZH2 vector and miR-139-5p inhibitor).

Prior to transfection, cells in the logarithmic phase of growth were seeded into a 6-well plate. When cell density reached 80-90%, the cells were transferred to serum-free Opti-MEM (Gibco Company, USA) for subsequent culture. Transfection was carried out in accordance with the instructions of Lipofectamin 2000 (Invitrogen Inc., USA). Lipo solution (250 μl) comprising of 240 μl serum-free culture medium and 10 μl Lipo was incubated for 5 min. The plasmid solution (20 μl) was composed of 20 μl serum-free culture medium and 4 μg plasmid. Then, the two mixed solutions were allowed to stand at room temperature for 20 min, and added into the well drop- by-drop, and the plate was shaken gently. After that, the cells were incubated in a humidified incubator with 5% CO_2 in air at 37℃ for 5-6 h, and cultured for another 24-48 h in complete medium for subsequent experiments.

Western blot analysis

Total protein content of samples was extracted using lysate (C0481, Sigma-Aldrich Chemical Company, USA). The concentration of proteins extracted using lysate (C0481, Sigma-Aldrich Chemical Company, USA) was determined using a bicinchoninic acid (BCA). Next, 20 μg of loading sample was added to each well, mixed with the loading buffer, boiled for 5 min, ice-bathed, centrifuged, and added into each lane for electrophoresis separation by pipettes, with equal amounts added in each well. Next, the target proteins were transferred onto a poly-vinylidene fluoride (PVDF) membrane. The membrane was blocked with 5% skimmed milk powder for 1 h, and incubated with the following primary antibodies: rabbit anti-human EZH2 (dilution ratio of 1 : 1500, ab186006), rabbit anti-human N-cadherin (dilution ratio of 1 : 1000, ab18203), rabbit anti-human Vimentin (dilution ratio of 1 : 2000, ab92547), rabbit anti-human E-cadherin antibody (dilution ratio of 1 : 15000, ab40772), rabbit anti-human H3K27me3 (dilution ratio of 1 : 1000, ab192985), ZEB1 (dilution ratio of 1 : 1000, ab124512), and ZEB2 (dilution ratio of 1 : 500, ab138222) at 4℃ overnight. All aforementioned antibodies were provided by Abcam Inc. (USA). The following day, after rinsing with tris-buffered saline tween 20 (TBST) three times (5 min each time), the membrane was incubated with the goat anti-rabbit IgG antibody (dilution ratio of 1 : 500, Cwbiotech Co., Ltd, China) at room temperature for 1.5 h. Then, the membrane was rinsed with TBST. Enhanced chemiluminescence (ECL) (Beijing Solarbio Science & Technology Co., Ltd., China) was employed for protein coloration. β-actin was regarded as the internal reference. The primary antibody was mouse anti-β-actin (dilution ratio of 1 : 500) and the secondary antibody was HRP labeled goat anti-rat IgG (dilution ratio of 1 : 2000), both of which were purchased from Cwbiotech Co., Ltd, China. Incubation was carried out using the above-mentioned methods. The ratios of absorbance

value of EZH2, N-cadherin, Vimentin, E-cadherin, H3K27me3, and ZEB1/2 to that of β-actin were analyzed using the Image J software in order to calculate the relative expression of EZH2, N-cadherin, Vimentin, E-cadherin, H3K27me3, and ZEB1/2 for gray value analysis. Each experiment was repeated three times.

3-(4,5-dimethyl-2-thiazolyl)-2,5-diphenyl-2-H-tetrazolium bromide (MTT) assay

Mesothelial cells in the logarithmic phase of growth were seeded in a 96-well plate (cell density of 1×10^5 cells/ml). There were a total of 8 replicates in each group with 100 μl in each well. Next, the cells were cultured in a humidified incubator with 5% CO_2 in air at 37℃ for 24 h followed by further culturing in 1% fetal calf serum (FCS) 1640 medium overnight. Then, 2 mg/ml MTT solution was added into each group for another 4-h culture. Dimethyl sulfoxide (DMSO) (Beijing Chemical Factory, China) was added and shaken for 10 min to fully dissolve the crystals. The optical density (OD) value of each well at 570 nm wavelength was measured using a microplate reader (680, Bio-Rad, Inc., USA). Subsequently, MTT curves were drawn with OD value as the Y-axis and time points as X-axis. Each experiment was repeated three times.

Scratch test

A total of six 6-well plates were selected, and cells were grouped according to the corresponding incubation group in each plate. Behind each plate, a marker pen was used to draw a uniform line every 0.5-1 cm crossing the well, and at least 5 lines were drawn per well. Then, each well was added with approximately 5×10^5 cells for overnight culture. On the 2nd day, a pipette's tip was used for scratching vertical lines onto the original lines. Next, the cells were rinsed with PBS three times with the removal of scratched-out cells, and cultured in serum-free medium in a humidified incubator with 5% CO_2 in air at 37℃ followed by observation at 0 h, 12 h and 24 h time intervals under an inverted microscope (magnified at × 40). Subsequently, photographs were obtained and the scratch distance was measured. Each experiment was repeated three times.

Transwell assay

The upper chamber was added with 60 μl 50 mg/L Matrigel (dilution ratio of 1:8, Sigma-Aldrich Chemical Company, USA). After air drying at room temperature, the remaining liquid in the plate was absorbed. Each chamber was added with 50 μl serum-free medium containing 10 g/L bovine serum albumin (BSA), and placed for 30 min at 37℃. Next, cells in the logarithmic phase of growth were adjusted to a density of 1×10^5 cells/ml using serum-free medium containing 10 g/L BSA, and 200 μl cell suspension was added into each chamber. Then, 500 μl medium containing 100 ml/L FBS was added into the lower chamber, and the 24-well plate was placed in a humidified incubator with 5% CO_2 in air at 37℃ for 24 h. After that, the cells on the PVDF membrane close to the inner side of chamber were extracted using a cotton swab. The chamber was taken out, and the cells were fixed in 95% alcohol at room temperature for 30 min, stained with Giemsa (Sigma-Aldrich Chemical Company, USA) for 20 min, and washed with running water for three times. Photographs were obtained under an inverted microscope (Olympus Optical Co., Ltd., Japan) with the cell number counted. Each experiment was repeated three times.

Cellular tumorigenicity in nude mice

BxPC-3 cells in the logarithmic phase of growth from each group were injected into the back of female BALB/c nude mice (age: 4-6 weeks). The mice were exposed to 8 Gy of X-rays when tumor volume reached 50 mm^3. The tumor volume was measured every 5 days after radiation exposure. The approximate volume of tumor was calculated according to the following formula: V (mm^3) = $A^2 \times B/2$ (A is long diameter, B is short diameter), which was later used to plot a tumor growth curve. Mice were executed 20 days after radiation exposure, and the grown tumors were resected and weighed. Each experiment was repeated three times.

Hematoxylin-eosin (HE) staining

The tumors in nude mice were collected, and then fixed with 10% neutral formalin for at least 24 h. Paraffin sections were dewaxed with xylene two times (10 min each time), dehydrated with gradient alcohol (100% for 5 min, 90% for 2 min and 70% for 2 min), and washed with distilled water for 2 min. Then, the samples were stained with hematoxylin for 7 min, and washed with running water to remove the extra dye liquor. Distilled water washing was repeated once. After treatment with 95% alcohol for 5 s, the specimens were stained with eosin for 1 min, dehydrated with gradient alcohol (100%, 95%, 75% and 50%) for two times (2 min each time), and cleared with xylene two times (5 min each time). In fume hood, the dried tissues were sealed with neutral balsam. Then, histopathological changes of tumors were observed under an optical microscope to confirm the occurrence of LNM.

Statistical analysis

Statistical analyses were performed using the SPSS 21.0 statistical software (IBM Corp., USA). Measurement data are presented as mean ± standard deviation. Each experiment was conducted for at least three times in order to obtain the mean value. The *t*-test was used to compare data between two groups, and one-way analysis of variance (ANOVA) was used for comparisons among multiple groups. $p < 0.05$ was indicative of significant difference, and $p < 0.01$ was indicative of highly significant difference.

RESULTS

EZH2 is highly expressed and miR-139-5p is poorly expressed in PC tissues

Initially, the results of immunohistochemical staining (Figs. 1A-1C) showed that the positive expression of EZH2 that exhibited as yellow or brown granules in the nuclei in tissues was found to be significantly higher in PC tissues (74.51%) compared to the adjacent normal tissues (29.42%) ($p < 0.05$). According to the expression of miR-139-5p in patients with PC, the patients were subsequently divided into

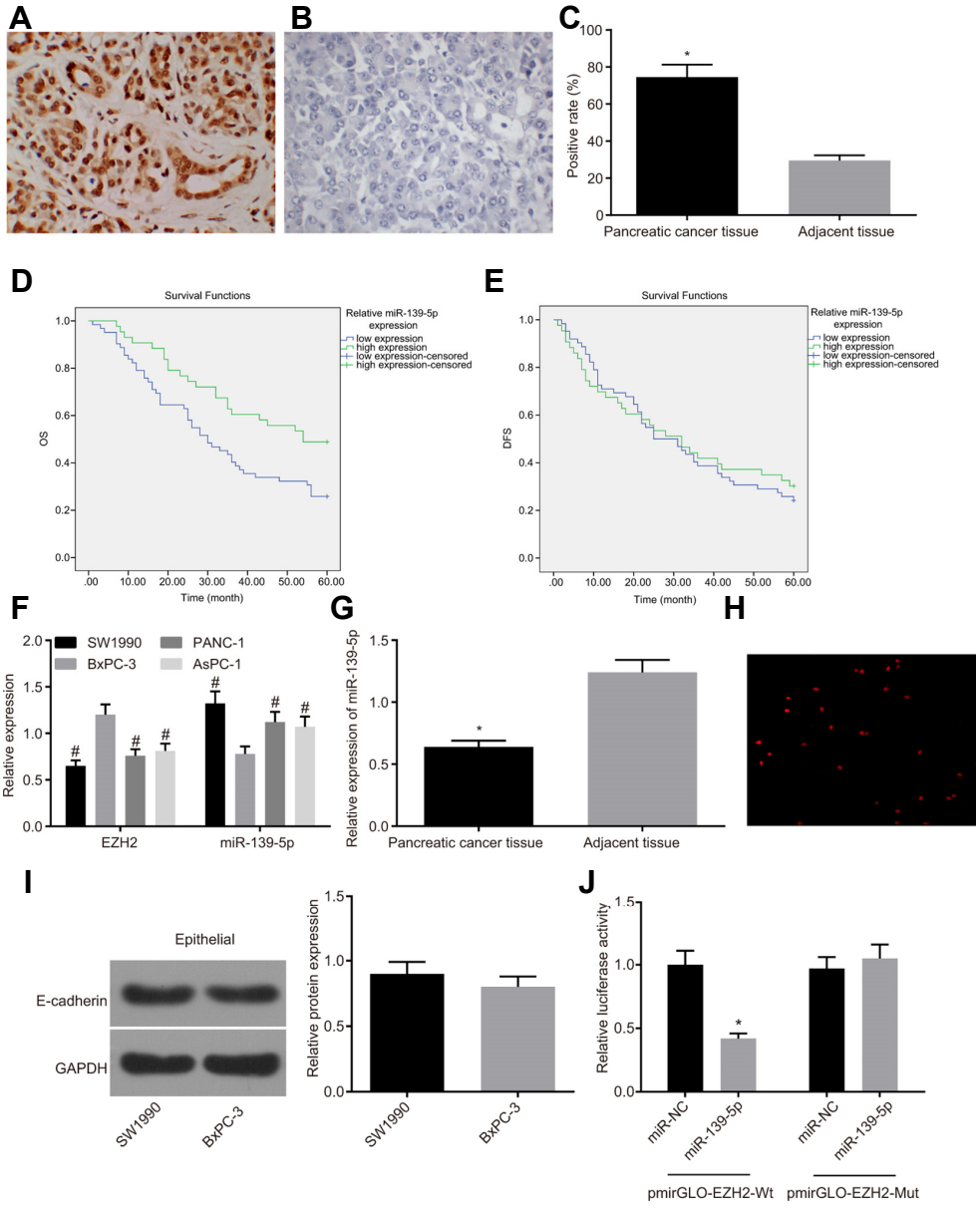

Fig. 1. EZH2 is highly expressed and miR-139-5p is poorly expressed in PC tissues. (A-C) Higher positive expression of EZH2 is observed in PC tissues (n = 105) as compared with adjacent normal tissues (n = 105), based on immunohistochemical staining (magnified at × 400); (D, E) The OS of the miR-139-5p high expression group is better than that in the miR-139-5p low expression group, and the DFS is not significantly different, based on Kaplan-Meier analysis (n = 105); (F) The BxPC-3 cell line with the highest expression of EZH2 and lowest expression of miR-139-5p is selected for subsequent experiments, based on detection of RT-qPCR in PC cell lines (n = 3); (G) miR-139-5p is poorly expressed in PC tissues compared to adjacent normal tissues (n = 105); Panel H, EZH2 is mainly located in the nucleus, based on immunofluorescence analysis (magnified at × 400) (n = 3); Panel I, the uniformed marker and phenotype of EMT in SW1990 and BxPC-3 cell lines are detected by Western blot assay; (J) The higher dual-luciferase activity of pmiR-139-5p-Mut than pmiR-139-5p-Wt, $*p < 0.05$, *vs.* the miR-NC group; $*p < 0.05$, *vs.* the adjacent normal tissues; $\#p < 0.05$, *vs.* the BxPC-3 cell line; the enumeration data are analyzed by chi-square test; the measurement data are analyzed by *t*-test; comparisons among multiple groups were performed using one-way ANOVA; PC, pancreatic cancer, miR-139-5p, microRNA-139-5p; EZH2, enhancer of zeste homolog 2; EMT, epithelial-mesenchymal transition; OS, overall survival; DFS, disease-free survival; NC, negative control; Mut, ,mutant; Mt, wide type.

the miR-139-5p high expression group and the miR-139-5p low expression group, and their survival curves were drawn using the Kaplan-Meier method. The log-rank test was performed to compare the disease-free survival (DFS) and overall survival (OS) between the two aforementioned groups. As shown in Figs. 1D and 1E, the survival of patients in the

miR-139-5p high expression group was better than those in the miR-139-5p low expression group, in addition to significant OS differences between the two groups ($p < 0.05$), whereas the DFS was not evidently different ($p > 0.05$). The results of RT-qPCR reflected that compared with BxPC-3 cell lines, the mRNA expression of EZH2 in PANC-1, AsPC-1 and SW1990 cell lines was found to be significantly decreased ($p < 0.05$), while that in miR-139-5p increased significantly ($p < 0.05$), therefore, the BxPC-3 cell line was selected for subsequent experimentation (Fig. 1F). Owing to the fact the expression of EZH2 was inversely proportional to miR-139-5p in SW1990 and BxPC-3 cell lines, we further identified the marker and phenotype of EMT by adopting E-cadherin for Western blot analysis (Xu et al., 2013). The SW1990 and BxPC-3 cell lines presented with the consistent marker and phenotype of EMT (Fig. 1I).

Compared with the adjacent normal tissues, miR-139-5p was found to be poorly expressed in PC tissues ($p < 0.05$) (Fig. 1G). In line with the results of immunohistochemical staining, the immunofluorescence assay showed that the fluorescence intensity in the cytoplasm was significantly weakened in comparison to the nucleus, indicating that the positive expression EZH2 was found in BxPC-3 cells and localized to the nucleus (Fig. 1H). The result of dual luciferase reporter gene assay revealed that compared with the NC group, the miR-139-5p mimic could significantly decrease the luciferase activity of pmirGLO-EZH2-Wt ($p < 0.05$), while no notable changes were observed in pmirGLO-EZH2-Mut, thus showing that miR-139-3p can bind to EZH2 (Fig. 1J). These results indicated high expression of EZH2 and low expression of miR-139-5p in PC tissues.

Expression of miR-139-5p and EZH2 are associated with clinicopathological features of PC patients

After assessing the expression of EZH2 and miR-139-5p in PC tissues, 105 PC cases were observed and analyzed, and we found that the expression levels of miR-139-5p and EZH2 were not correlated with age, sex and tumor location of patients with PC ($p > 0.05$). While low expressions of miR-139-5p and high expressions of EZH2 were observed in PC patients at stage III/IV, with LNM and highly-differentiated ones when compared with patients at stage II, without LNM and with low or moderately-differentiated ones ($p < 0.05$), as presented in Table 2. Therefore, it can be concluded that the expression of miR-139-5p and EZH2 expression are associated with the clinicopathological features of PC patients.

EZH2 suppresses miR-139-5p expression by up-regulating H3K27me3

Previous results showed that the expression level of miR-139-5p was negatively related to EZH2; meanwhile, EZH2 functions as a methyltransferase in regulating trimethylation of H3K27. Therefore, a chromatin immunoprecipitation assay was performed in order to verify whether miR-139-5p is regulated by H3K27me3. Accordingly, DNA fragments were processed with anti-H3K27me3 antibodies to obtain the recombinant fragments with those gene fragments that cannot combine with H3K27me3 eluted. Next, these

Table 2. The expression of miR-139-5p and EZH2 is associated with the clinical stage, lymph node metastasis and degree of tumor differentiation of patients with PC

Clinicopathological features	n	mRNA expression of EZH2	*p*	Relative expression of miR-139-5p	*p*
Gender					
Male	59	1.19 ± 0.10	0.354	0.79 ± 0.08	0.207
Female	46	1.21 ± 0.12		0.77 ± 0.08	
Age (years)					
≥ 50	58	1.21 ± 0.10	0.165	0.78 ± 0.08	0.526
< 50	47	1.18 ± 0.12		0.79 ± 0.08	
Tumor location					
Pancreatic head	64	1.19 ± 0.11	0.366	0.78 ± 0.08	0.999
Pancreatic tail	41	1.21 ± 0.11		0.78 ± 0.08	
Clinical stages					
II	34	1.11 ± 0.07		0.84 ± 0.06	
III	31	1.20 ± 0.07	< 0.001	0.80 ± 0.06	< 0.001
IV	40	1.28 ± 0.10		0.71 ± 0.05	
Degree of differentiation					
Lowly-differentiated	36	1.13 ± 0.11		0.84 ± 0.08	
Moderately differentiated	43	1.20 ± 0.07	< 0.001	0.77 ± 0.07	< 0.001
Highly-differentiated	26	1.30 ± 0.11		0.71 ± 0.06	
Lymph node metastasis					
No	56	1.14 ± 0.11	< 0.001	0.83 ± 0.08	< 0.001
Yes	49	1.26 ± 0.10		0.72 ± 0.06	

Notes: PC, pancreatic cancer; miR-139-5p, microRNA-139-5p; EZH2, enhancer of zeste homolog 2.

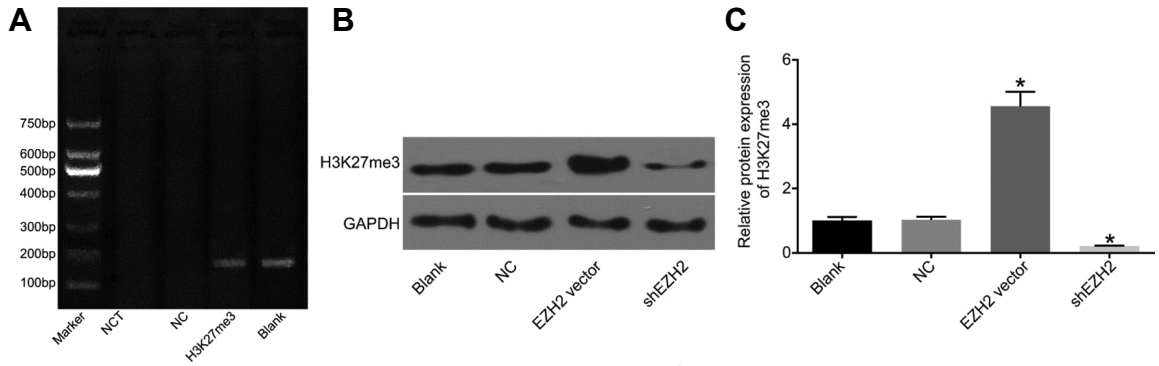

Fig. 2. miR-139-5p is negatively regulated by EZH2 by increased expression of H3K27me3, which is validated by RT-qPCR and ChIP. (A) The results of RT-qPCR and ChIP reveal that miR-139-5p is regulated by H3K27me3; (B) Over-expressed EZH2 functions to promote the protein expression of H3K27me3; (C) The statistical analysis for the effect of EZH2 on the protein expression of H3K27me3; $*p < 0.05$, *vs.* the NC group; NC, negative control; miR-139-5p, microRNA-139-5p; EZH2, enhancer of zeste homolog 2; RT-qPCR, reverse transcription quantitative polymerase chain reaction; ChIP, chromatin immunoprecipitation.

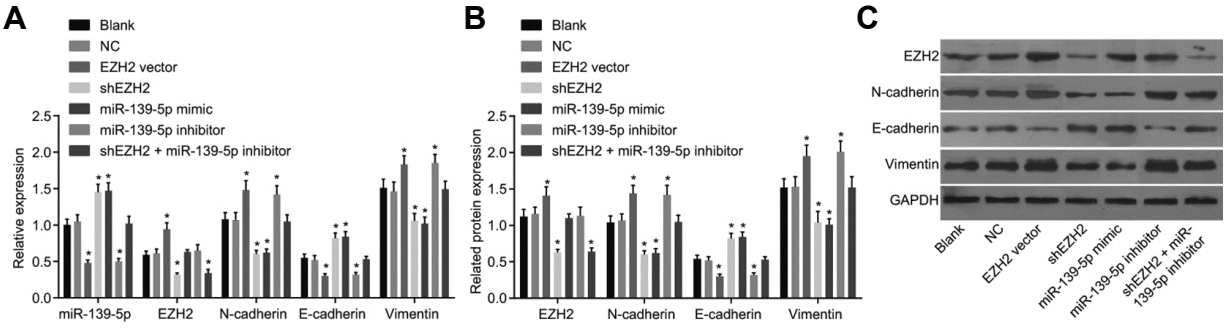

Fig. 3. Down-regulated expression of EZH2 and up-regulated expression of miR-139-5p suppresses EMT in PC cells. RT-qPCR (A) and Western blot analysis (B, C) are employed to determine the expression of miR-139-5p, EZH2, N-cadherin, Vimentin and E-cadherin. Down-regulated EZH2 expression and up-regulated expression of miR-139-5p enhance gene expressions of epithelial lineage-related marker (E-cadherin) and suppress those of mesenchymal cells-related markers (N-cadherin and Vimentin). $*p < 0.05$, *vs.* the blank and NC group; n = 3; the measurement data are analyzed by *t*-test; PC, pancreatic cancer, miR-139-5p, microRNA-139-5p; EZH2, enhancer of zeste homolog 2; EMT, epithelial-mesenchymal transition.

recycled fragments were detected by PCR, and the results revealed that H3K27me3 antibody enriched with the miR-139-5p gene fragment, in which a 166 bp band was found, whereas a brighter band of the total DNA was observed in the blank group, in addition to no bands in the blank and NC groups (Fig. 2A). At the same time, the influence of different expression levels of EZH2 on H3K27me3 expression were detected using RT-qPCR and Western blot assay: compared with the NC group, over-expression of EZH2 promoted the expression of H3K27me3 in BxPC-3 cells, while down-regulation of EZH2 worked to significantly inhibit the expression of H3K27me3 ($p < 0.05$) (Figs. 2B and 2C). The results indicated that miR-139-5p is negatively regulated by EZH2 through the up-regulation of H3K27me3.

Down-regulation of EZH2 and up-regulation of miR-139-5p inhibit EMT in PC cells

Following the analysis of the regulatory relationship between miR-139-5p and EZH2, RT-qPCR (Fig. 3A) and Western blot analysis (Figs. 3B and 3C) were employed in order to determine the expression of miR-139-5p, EZH2, N-cadherin, Vimentin, E-cadherin, ZEB1 and ZEB2 in each group. There were no significant differences in the expression levels of miR-139-5p, EZH2, N-cadherin, Vimentin, E-cadherin, ZEB1 and ZEB2 between the blank and NC groups, and no difference in the expression levels of N-cadherin, Vimentin and E-cadherin were observed between the EZH2 vector and miR-139-5p inhibitor groups, and between the shEZH2 and miR-139-5p mimic groups ($p > 0.05$). Compared with the blank and NC groups, the mRNA and protein expression of N-cadherin, Vimentin, ZEB1 and ZEB2 were found to be increased while E-cadherin levels were decreased in the EZH2 vector and miR-139-5p inhibitor groups; but an opposite trend was observed in the shEZH2 and miR-139-5p mimic groups ($p < 0.05$). There were no obvious changes in the mRNA and protein expressions of N-cadherin, Vimentin, E-cadherin, ZEB1 and ZEB2 in the shEZH2 + miR-139-5p inhibitor groups ($p > 0.05$), where the expression of EZH2 was

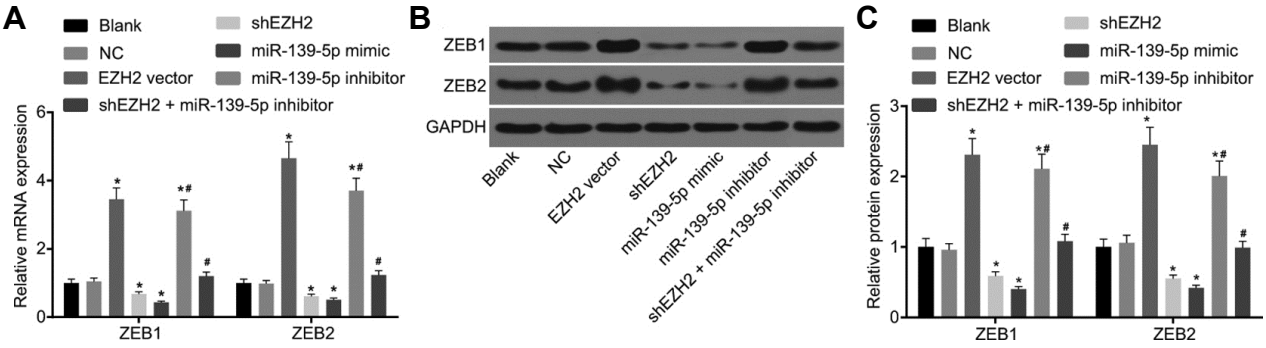

Fig. 4. Over-expressed EZH2 promotes the expression of ZEB1 and ZEB2. (A) mRNA expression of ZEB1 and ZEB2 in different groups; (B) Protein expression of ZEB1 and ZEB2 in different groups; $*p < 0.05$, *vs.* the NC group; $\#p < 0.05$, *vs.* the miR-139-5p inhibitor group; NC, negative control; EZH2, enhancer of zeste homolog 2.

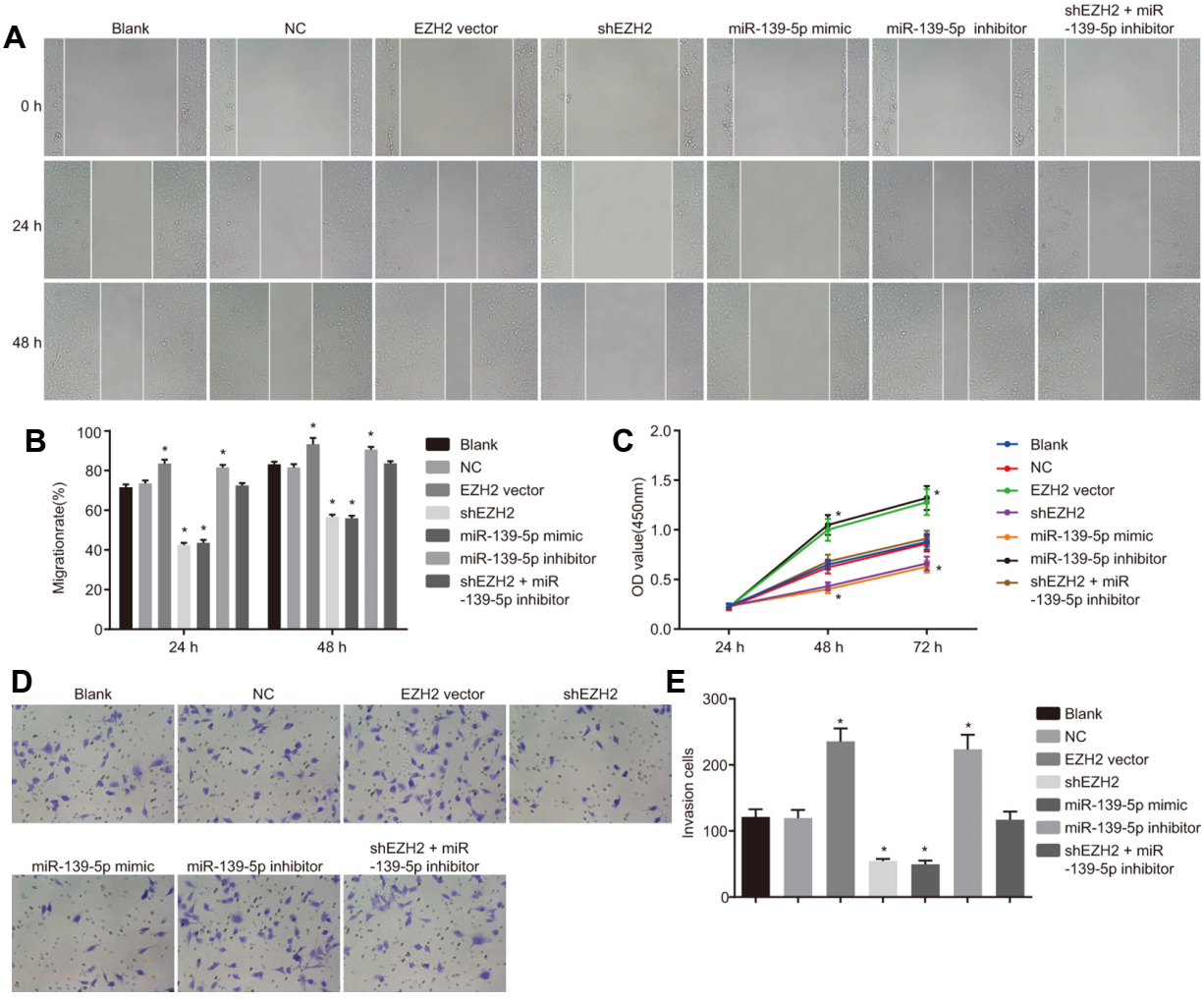

Fig. 5. Down-regulated expression of EZH2 expression and up-regulated expression of miR-139-5p repress migration, proliferation and invasion abilities of PC cells. (A) The effect of EZH2 expression and miR-139-5p expression on PC cell migration detected by scratch test (magnified at × 100); (B) The migration rate of PC cells at time points of 24 h and 48 h; (C) The effect of EZH2 expression and miR-139-5p expression on PC cell proliferation detected by MTT assay; (D) The effect of EZH2 expression and miR-139-5p expression on PC cell invasion detected by Transwell test; (E) The number of invading PC cells; $*p < 0.05$, *vs.* the blank and NC group; n = 3; the measurement data are analyzed by *t*-test; PC, pancreatic cancer, miR-139-5p, microRNA-139-5p; EZH2, enhancer of zeste homolog 2; NC, negative control.

found to be decreased ($p < 0.05$) (Figs. 3 and 4). In comparison to the blank and NC groups, there were no differences in the expression of EZH2 in the miR-139-5p mimic and miR-139-5p inhibitor groups ($p > 0.05$), while the expression of EZH2 was found to be elevated in the EZH2 vector group but reduced in the shEZH2 group ($p < 0.05$). These aforementioned results reflect that suppressed EZH2 or over-expressed miR-139-5p promotes the gene expressions of epithelial lineage-related marker while inhibits those of mesenchymal cells-related markers.

Down-regulation of EZH2 and up-regulation of of miR-139-5p impede migration, proliferation and invasion abilities of PC cells

Next, in order to observe the regulatory mechanism of EZH2 on migration (Figs. 5A and 5B), proliferation (Fig. 5C) and invasion (Figs. 5D and 5E) of PC cells, we conducted a scratch test, MTT assay and Transwell test, respectively. There were no significant differences in cell migration, proliferation and invasion abilities between the blank and NC groups, between the EZH2 vector and miR-139-5p inhibitor groups, and between the shEZH2 and miR-139-5p mimic groups ($p > 0.05$). Compared with the blank and NC groups, enhanced cell migration, proliferation and invasion abilities were found in the EZH2 vector group and miR-139-5p inhibitor groups ($p < 0.05$); an opposite trend was observed in the shEZH2 group and miR-139-5p mimic group ($p < 0.05$); while no significant changes of above mentioned cell abilities were found in the shEZH2 + miR-139-5p inhibitor group ($p > 0.05$). These findings indicated that suppressed EZH2 expression and over-expressed miR-139-5p inhibit proliferation, migration and invasion of PC cells.

Down-regulation of EZH2 and up-regulation of miR-139-5p reduce tumor formation and LNM of PC

Finally, in order to verify the aforementioned results, an animal experiment was carried out, by which the pancreatic cancer cell suspensions were transfected into nude mice to observe the changes of tumor formation and body weight. The results showed that there were no significant differences in tumor volume between the blank and NC groups, between the EZH2 vector and miR-139-5p inhibitor groups, and between the shEZH2 and miR-139-5p mimic groups ($p > 0.05$). Compared with the blank and NC groups, significantly increased tumor volume on the 3rd week ($p < 0.05$) and the 4th week ($p < 0.01$) was found in the EZH2 vector group and miR-139-5p inhibitor groups; an opposite trend was observed in the shEZH2 cell group and miR-139-5p mimic groups ($p < 0.05$); while no significant changes of tumor volume were found in the shEZH2 + miR-139-5p inhibitor group ($p > 0.05$) (Figs. 6A-6C). Histological observation carried out using HE staining reflected that there were

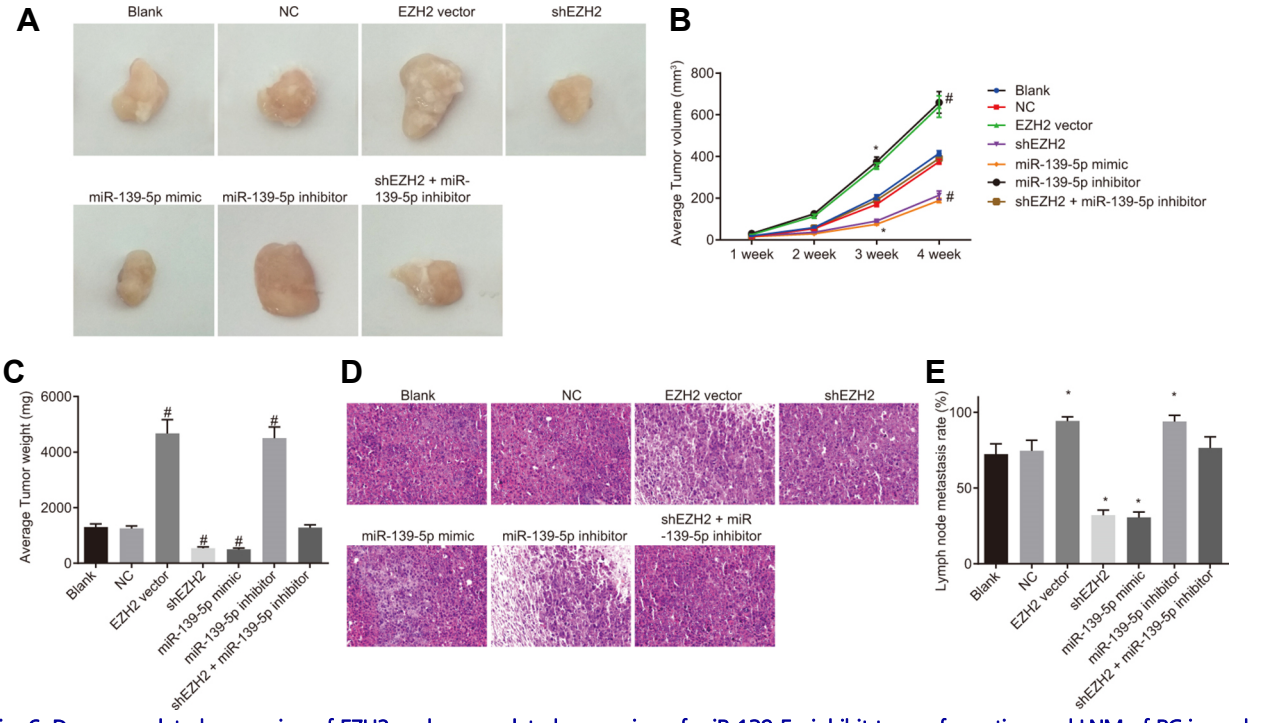

Fig. 6. Down-regulated expression of EZH2 and up-regulated expression of miR-139-5p inhibit tumor formation and LNM of PC in nude mice. (A) The tumors of nude mice in each group to identify cellular tumorigenicity; (B) Average tumor volume of nude mice is reduced when treated with shEZH2 and miR-139-5p mimic; (C) Average tumor weight of mice is reduced when treated with shEZH2 and miR-139-5p mimic; (D) LNM observed by hematoxylin-eosin staining; (E) The LNM rate is reduced when treated with shEZH2 and miR-139-5p mimic; $*p < 0.05$, *vs.* the blank and NC group; $\#p < 0.01$, *vs.* the blank and NC group; n = 3; the measurement data are analyzed by *t*-test; PC, pancreatic cancer, miR-139-5p, microRNA-139-5p; EZH2, enhancer of zeste homolog 2; LNM, lymph node metastasis.

visible metastatic lesions in the blank and NC groups, less in the EZH2 vector and miR-139-5p inhibitor groups, and much more in the shEZH2 and miR-139-5p mimic groups. Compared with the blank and NC groups, higher LNM rates was found in the EZH2 vector and miR-139-5p inhibitor groups ($p < 0.05$), while lower rates were observed in the shEZH2 and miR-139-5p mimic group ($p < 0.05$) (Figs. 6D and 6E). The aforementioned results verified that suppressed EZH2 expression and over-expressed miR-139-5p inhibit tumor formation and LNM of PC in nude mice.

DISCUSSION

Pancreatic cancer (PC) is characterized by extremely poor prognosis owing to early recurrence and metastasis (Liu et al., 2013), and increasing evidence supports the crucial role of miR-139-5p in tumor suppression (Shen et al., 2014). The current study revealed the effect of EZH2/miR-139-5p axis in PC progression, in which down-regulation of EZH2 and up-regulation of miR-139-5p inhibited EMT and LNM.

We initially determined that miR-139-5p was poorly expressed, and EZH2 was highly expressed in PC, which were further closely related to advanced TNM stages, LNM, distant metastases, in addition to unfavorable prognoses of patients. In addition, the expression levels of EZH2 and miR-139-5p were found to be significantly associated with the clinicopathological features (Stage III/IV, LNM and highly-differentiated tumors) of patients with PC. EZH2, a catalytic subunit of PRC2, is an oncogenic protein that epigenetically silences expressions of diverse tumor suppressor mRNAs such as miR-139-5p, miR-125b, miR-101, let-7c, and miR-200b, and is commonly increased in human cancers such as hepatocellular carcinoma (Au et al., 2012). Interestingly, a previous study revealed that EZH2 is abundantly increased in PC (Hu et al., 2018), and aberrant nuclear accumulation of EZH2 promotes carcinogenesis, accelerates liver metastasis and facilitates cancer stem cell maintenance in PC cells (Chen et al., 2010). In addition, it was further reported that EZH2 promotes cancer metastasis via tumor suppressor miRNAs by establishing control of pathways related to cell motility and metastasis (Au et al., 2012). Furthermore, the inhibition of EZH2 can sensitize patients with PC to chemotherapy (Cao et al., 2008).

Our ChIP data argued that miR-139-5p is definitely negatively regulated by EZH2 through H3K27me3. Interestingly, a previous study reported that EZH2 represses tumor suppressor genes via tirmethylation of H3K27 (Reijm et al., 2014). Ma et al. (2017) have demonstrated that EZH2 is capable of mediating H3K27me3 in PC cells. Furthermore, a previous study demonstrated that inhibition of EZH2 notably promotes the miR-99a/let7c/125b-2 cluster with the involvement of androgen (Sun et al., 2014), which supports our result that EZH2 could indirectly down-regulate miR-139-5p. Moreover, another miRNA, namely miR-125b, capable of regulating EMT in cancer cells such as paclitaxel-resistant breast cancer cells, has also been reported to be enriched in H3K27me3, and thus, may possess similar regulatory function on PC as EZH2, which requires a future study (Xu et al., 2013; Yang et al., 2015).

Employing loss-of-function and gain-of-function approaches, we identified that EZH2 and miR-139-5p play a key role in PC cell proliferation, migration, invasion as well as pancreatic tumor formation and LNM. In the current study, deletion of EZH2 or up-regulation of miR-139-5p significantly weakened PC cell growth ability, decreased cell migration and invasion capacity, and further inhibited tumor formation and metastasis, and vice versa in cells with over-expressed EZH2 or lowly-expressed miR-139-5p. MiRNAs function as oncogenes or tumor suppressors in cellular processes during tumor formation (Di Leva and Croce, 2010). Furthermore, miR-139-5p has been reported to exert an inhibitory effect on the progression of various cancers such as gastric, breast, bladder and hepatocellular carcinoma (Hu et al., 2017; Zhang et al., 2015). A previous study indicated that miR-139-5p can repress colorectal cancer growth, metastasis, and chemoresistance by regulating several genes such as NOTCH1, BCL2, and AMFR (Bian et al., 2017). Furthermore, Li et al. (2017) revealed that decreased miR-139-5p expression leads to an anti-apoptotic effect in diabetic rat pancreas, which is in accordance with our results.

Endothelial dysfunction is a known major risk factor for PC, and EMT, an important pathophysiological event, is closely related to endothelial dysfunction (Zhang et al., 2018). With the progression of EMT, cancer cells transform from adherent and polarized epithelial cells to invasive mesenchymal cell phenotypes, which contributes to early dissemination of primary tumor cells and metastatic spread (Mody et al., 2016; Zhang et al., 2017). Accumulating data have indicated that EMT leads to escalating cell migration in various tumors including PC (Chen et al., 2017). Furthermore, it has been elucidated that cells presenting with a loss of E-cadherin are prone to EMT induction by means of various growth factors (Kim et al., 2002). In the current study, we have demonstrated that miR-139-5p and EZH2 play vital roles in EMT formation, since silencing of EZH2 or up-regulating miR-139-5p inhibited the formation of the EMT phenotype, and vice versa in cells with EZH2 over-expression or low expression of miR-139-5p. In consistency with our study, Chen et al. (2017) also mentioned that E-cadherin was weakly expressed in PC tissue samples in comparison with normal tissue samples. Moreover, the promotion of EMT by the transcription factors ZEB1 and ZEB2 was formerly revealed with the complemented information showing that the repression of ZEB1 and ZEB2 by p53 works to inhibit EMT (Kim et al., 2011).

In summary, the current study shows that EZH2 regulates the expression of miR-139-5p via H3K27me3, and the EZH2/miR-139-5p axis participates in the progression of PC, whereby down-regulation of EZH2 and up-regulation of miR-139-5p repress EMT and LNM of PC. Therefore, it is possible that therapeutic interventions of EZH2 and restoration of miR-139-5p may lead to improved prognosis against PC aggression.

ACKNOWLEDGMENTS

We would like to acknowledge the reviewers for their helpful comments on this paper.

REFERENCES

Adsay, N.V., Bagci, P., Tajiri, T., Oliva, I., Ohike, N., Balci, S., Gonzalez, R.S., Basturk, O., Jang, K.T., and Roa, J.C. (2012). Pathologic staging of pancreatic, ampullary, biliary, and gallbladder cancers: pitfalls and practical limitations of the current AJCC/UICC TNM staging system and opportunities for improvement. Semin Diagn Pathol. *29*, 127-141.

Au, S.L., Wong, C.C., Lee, J.M., Fan, D.N., Tsang, F.H., Ng, I.O., and Wong, C.M. (2012). Enhancer of zeste homolog 2 epigenetically silences multiple tumor suppressor microRNAs to promote liver cancer metastasis. Hepatology *56*, 622-631.

Bian, Z., Zhang, J., Li, M., Feng, Y., Yao, S., Song, M., Qi, X., Fei, B., Yin, Y., Hua, D., et al. (2017). Long non-coding RNA LINC00152 promotes cell proliferation, metastasis, and confers 5-FU resistance in colorectal cancer by inhibiting miR-139-5p. Oncogenesis *6*, 395.

Cao, Q., Yu, J., Dhanasekaran, S.M., Kim, J.H., Mani, R.S., Tomlins, S.A., Mehra, R., Laxman, B., Cao, X., Yu, J., et al. (2008). Repression of E-cadherin by the polycomb group protein EZH2 in cancer. Oncogene *27*, 7274-7284.

Chen, L., Ma, C., Bian, Y., Shao, C., Wang, T., Li, J., Chong, X., Su, L., and Lu, J. (2017). Aberrant expression of STYK1 and E-cadherin confer a poor prognosis for pancreatic cancer patients. Oncotarget *8*, 111333-111345.

Chen, Y., Xie, D., Yin Li, W., Man Cheung, C., Yao, H., Chan, C.Y., Chan, C.Y., Xu, F.P., Liu, Y.H., Sung, J.J., et al. (2010). RNAi targeting EZH2 inhibits tumor growth and liver metastasis of pancreatic cancer *in vivo*. Cancer Lett. *297*, 109-116.

Di Leva, G., and Croce, C.M. (2010). Roles of small RNAs in tumor formation. Trends Mol Med. *16*, 257-267.

Ebrahimi, S., Hosseini, M., Ghasemi, F., Shahidsales, S., Maftouh, M., Akbarzade, H., Parizadeh, S.A., Hassanian, S.M., and Avan, A. (2016). Circulating microRNAs as potential diagnostic, prognostic and therapeutic targets in pancreatic cancer. Curr. Pharm. Des. *22*, 6444-6450.

Feng, H., Wang, Y., Su, J., Liang, H., Zhang, C.Y., Chen, X., and Yao, W. (2016). MicroRNA-148a suppresses the proliferation and migration of pancreatic cancer cells by down-regulating ErbB3. Pancreas *45*, 1263-1271.

Gayral, M., Jo, S., Hanoun, N., Vignolle-Vidoni, A., Lulka, H., Delpu, Y., Meulle, A., Dufresne, M., Humeau, M., Chalret du Rieu, M., et al. (2014). MicroRNAs as emerging biomarkers and therapeutic targets for pancreatic cancer. World J. Gastroenterol. *20*, 11199-11209.

Han, T., Jiao, F., Hu, H., Yuan, C., Wang, L., Jin, Z.L., Song, W.F., and Wang, L.W. (2016). EZH2 promotes cell migration and invasion but not alters cell proliferation by suppressing E-cadherin, partly through association with MALAT-1 in pancreatic cancer. Oncotarge. *7*, 11194-11207.

Hartwig, W., and Buchler, M.W. (2013). Pancreatic cancer: current options for diagnosis, staging and therapeutic management. Gastrointest Tumors *1*, 41-52.

Hu, W., Jia, X., Gao, Y., and Zhang, Q. (2018). Chaetospirolactone reverses the apoptotic resistance towards TRAIL in pancreatic cancer. Biochem. Biophys. Res. Commun. *495*, 621-628.

Hu, Y., Deng, C., Zhang, H., Zhang, J., Peng, B., and Hu, C. (2017). Long non-coding RNA XIST promotes cell growth and metastasis through regulating miR-139-5p mediated Wnt/beta-catenin signaling pathway in bladder cancer. Oncotarget *8*, 94554-94568.

Jin, X., Yang, C., Fan, P., Xiao, J., Zhang, W., Zhan, S., Liu, T., Wang, D., and Wu, H. (2017). CDK5/FBW7-dependent ubiquitination and degradation of EZH2 inhibits pancreatic cancer cell migration and invasion. J. Biol. Chem. *292*, 6269-6280.

Kim, K., Lu, Z., and Hay, E.D. (2002). Direct evidence for a role of beta-catenin/LEF-1 signaling pathway in induction of EMT. Cell Biol. Int. *26*, 463-476.

Kim, T., Veronese, A., Pichiorri, F., Lee, T.J., Jeon, Y.J., Volinia, S., Pineau, P., Marchio, A., Palatini, J., Suh, S.S., et al. (2011). p53 regulates epithelial-mesenchymal transition through microRNAs targeting ZEB1 and ZEB2. J. Exp. Med. *208*, 875-883.

Li, J., Su, L., Gong, Y.Y., Ding, M.L., Hong, S.B., Yu, S., and Xiao, H.P. (2017). Downregulation of miR-139-5p contributes to the antiapoptotic effect of liraglutide on the diabetic rat pancreas and INS-1 cells by targeting IRS1. PLoS One *12*, e0173576.

Li, Q., Liang, X., Wang, Y., Meng, X., Xu, Y., Cai, S., Wang, Z., Liu, J., and Cai, G. (2016). miR-139-5p Inhibits the Epithelial-Mesenchymal Transition and Enhances the Chemotherapeutic Sensitivity of Colorectal Cancer Cells by Downregulating BCL2. Sci. Rep. *6*, 27157.

Liu, C., Cheng, H., Shi, S., Cui, X., Yang, J., Chen, L., Cen, P., Cai, X., Lu, Y., Wu, C., et al. (2013). MicroRNA-34b inhibits pancreatic cancer metastasis through repressing Smad3. Curr. Mol. Med. *13*, 467-478.

Livak, K.J., and Schmittgen, T.D. (2001). Analysis of relative gene expression data using real-time quantitative PCR and the 2(-Delta Delta C(T)) Method. Methods *25*, 402-408.

Ma, Z., Huang, H., Wang, J., Zhou, Y., Pu, F., Zhao, Q., Peng, P., Hui, B., Ji, H., and Wang, K. (2017). Long non-coding RNA SNHG15 inhibits P15 and KLF2 expression to promote pancreatic cancer proliferation through EZH2-mediated H3K27me3. Oncotarget *8*, 84153-84167.

Miao, F., Zhu, J., Chen, Y., Tang, N., Wang, X., and Li, X. (2016). MicroRNA-183-5p promotes the proliferation, invasion and metastasis of human pancreatic adenocarcinoma cells. Oncol. Lett. *11*, 134-140.

Mody, H.R., Hung, S.W., AlSaggar, M., Griffin, J., and Govindarajan, R. (2016). Inhibition of S-adenosylmethionine-dependent methyltransferase attenuates TGFβ1-Induced EMT and metastasis in pancreatic cancer: putative roles of miR-663a and miR-4787-5p. Mol. Cancer Res. *14*, 1124-1135.

Ougolkov, A.V., Bilim, V.N., and Billadeau, D.D. (2008). Regulation of pancreatic tumor cell proliferation and chemoresistance by the histone methyltransferase enhancer of zeste homologue 2. Clin. Cancer Res. *14*, 6790-6796.

Qi, W., Zhao, K., Gu, J., Huang, Y., Wang, Y., Zhang, H., Zhang, M., Zhang, J., Yu, Z., Li, L., et al. (2017). An allosteric PRC2 inhibitor targeting the H3K27me3 binding pocket of EED. Nat. Chem. Biol. *13*, 381-388.

Reijm, E.A., Timmermans, A.M., Look, M.P., Meijer-van Gelder, M.E., Stobbe, C.K., van Deurzen, C.H., Martens, J.W., Sleijfer, S., Foekens, J.A., Berns, P.M., et al. (2014). High protein expression of EZH2 is related to unfavorable outcome to tamoxifen in metastatic breast cancer. Ann. Oncol. *25*, 2185-2190.

Sclafani, F., Iyer, R., Cunningham, D., and Starling, N. (2015). Management of metastatic pancreatic cancer: Current treatment options and potential new therapeutic targets. Crit. Rev. Oncol. Hematol. *95*, 318-336.

Shen, K., Mao, R., Ma, L., Li, Y., Qiu, Y., Cui, D., Le, V., Yin, P., Ni, L., and Liu, J. (2014). Post-transcriptional regulation of the tumor suppressor miR-139-5p and a network of miR-139-5p-mediated mRNA interactions in colorectal cancer. FEBS J. *281*, 3609-3624.

Siegel, R.L., Miller, K.D., and Jemal, A. (2017). Cancer Statistics, 2017. CA Cancer J. Clin. *67*, 7-30.

Sun, D., Layer, R., Mueller, A.C., Cichewicz, M.A., Negishi, M., Paschal, B.M., and Dutta, A. (2014). Regulation of several androgen-induced genes through the repression of the miR-99a/let-7c/miR-125b-2 miRNA cluster in prostate cancer cells. Oncogene *33*, 1448-

1457.

Sun, C., Sang, M., Li, S., Sun, X., Yang, C., Xi, Y., Wang, L., Zhang, F., Bi, Y., Fu, Y., et al. (2015). Hsa-miR-139-5p inhibits proliferation and causes apoptosis associated with down-regulation of c-Met. Oncotarget *6*, 39756-39792.

Wang, Y., Li, J., Xu, C., and Zhang, X. (2017). MicroRNA-139-5p inhibit cell proliferation and invasion by targeting RHO-associated coiled-coil containing protein kinase 2 in ovarian cancer. Oncol. Res. doi: 10.3727/096504017X14974343584989. [Epub ahead of print].

Xu, J., Zhu, W., Xu, W., Yao, W., Zhang, B., Xu, Y., Ji, S., Liu, C., Long, J., Ni, Q., et al. (2013). Up-regulation of MBD1 promotes pancreatic cancer cell epithelial-mesenchymal transition and invasion by epigenetic down-regulation of E-cadherin. Curr. Mol. Med. *13*, 387-400.

Yang, Q., Wang, Y., Lu, X., Zhao, Z., Zhu, L., Chen, S., Wu, Q., Chen, C., and Wang, Z. (2015). MiR-125b regulates epithelial-mesenchymal transition via targeting Sema4C in paclitaxel-resistant breast cancer cells. Oncotarget *6*, 3268-3279.

Yonemori, M., Seki, N., Yoshino, H., Matsushita, R., Miyamoto, K., Nakagawa, M., and Enokida, H. (2016). Dual tumor-suppressors miR-139-5p and miR-139-3p targeting matrix metalloprotease 11 in bladder cancer. Cancer Sci. *107*, 1233-1242.

Zhang, H.D., Jiang, L.H., Sun, D.W., Li, J., and Tang, J.H. (2015). MiR-139-5p: promising biomarker for cancer. Tumour Biol. *36*, 1355-1365.

Zhang, Z., Che, X., Yang, N., Bai, Z., Wu, Y., Zhao, L., and Pei, H. (2017). miR-135b-5p Promotes migration, invasion and EMT of pancreatic cancer cells by targeting NR3C2. Biomed. Pharmacother. *96*, 1341-1348.

Zhang, J., Zhang, L., Li, C., Yang, C., Li, L., Song, S., Wu, H., Liu, F., Wang, L., and Gu, J. (2018). LOX-1 is a poor prognostic indicator and induces epithelial-mesenchymal transition and metastasis in pancreatic cancer patients. Cell Oncol (Dordr). *41*, 73-84.